JGR Biogeosciences

RESEARCH ARTICLE
10.1029/2022JG007325

Key Points:

- Differences in parent material were associated with differences in rates of Fe(III) reduction but not C mineralization
- Mixotrophic ability of many Fe(III)-reducers may partially explain the lack of pattern observed
- Soil chemistry may exert stronger controls over dissimilatory Fe(III)-reduction than microbial community composition

Supporting Information:

Supporting Information may be found in the online version of this article.

Correspondence to:

C. C. Reed,
cody.reed@unr.edu

Citation:

Reed, C. C., Dunham-Cheatham, S. M., Castle, S. C., Vuono, D. C., & Sullivan, B. W. (2023). The contribution of Fe(III) reduction to soil carbon mineralization in montane meadows depends on soil chemistry, not parent material or microbial community. *Journal of Geophysical Research: Biogeosciences*, *128*, e2022JG007325. https://doi.org/10.1029/2022JG007325

Received 6 DEC 2022
Accepted 18 APR 2023

Author Contributions:

Conceptualization: Cody C. Reed, Benjamin W. Sullivan
Formal analysis: Cody C. Reed, Sarrah M. Dunham-Cheatham, Sarah C. Castle, David C. Vuono, Benjamin W. Sullivan
Funding acquisition: Benjamin W. Sullivan
Investigation: Cody C. Reed, Sarrah M. Dunham-Cheatham, Benjamin W. Sullivan
Methodology: Cody C. Reed, Sarrah M. Dunham-Cheatham, Sarah C. Castle, David C. Vuono, Benjamin W. Sullivan
Project Administration: Cody C. Reed, Sarrah M. Dunham-Cheatham, Benjamin W. Sullivan
Resources: Sarrah M. Dunham-Cheatham, Benjamin W. Sullivan

The Contribution of Fe(III) Reduction to Soil Carbon Mineralization in Montane Meadows Depends on Soil Chemistry, Not Parent Material or Microbial Community

Cody C. Reed[1], Sarrah M. Dunham-Cheatham[2], Sarah C. Castle[3], David C. Vuono[4], and Benjamin W. Sullivan[1,5]

[1]Department of Natural Resources and Environmental Science, University of Nevada, Reno, Reno, NV, USA, [2]College of Agriculture, Biotechnology & Natural Resources, University of Nevada, Reno, Reno, NV, USA, [3]Department of Plant Pathology, University of Minnesota, St. Paul, MN, USA, [4]Department of Civil and Environmental Engineering, Colorado School of Mines, Golden, CO, USA, [5]The Global Water Center, University of Nevada, Reno, Reno, NV, USA

Abstract The long-term stability of soil carbon (C) is strongly influenced by organo-mineral interactions. Iron (Fe)-oxides can both inhibit microbial decomposition by providing physicochemical protection for organic molecules and enhance rates of C mineralization by serving as a terminal electron acceptor, depending on redox conditions. Restoration of floodplain hydrology in montane meadows has been proposed as a method of sequestering C for climate change mitigation. However, dissimilatory microbial reduction of Fe(III) could lead to C losses under increased reducing conditions. In this study, we explored variations in Fe-C interactions over a range of redox conditions and in soils derived from two distinct parent materials to elucidate biochemical and microbial controls on soil C cycling in Sierra Nevada montane meadows. Soils derived from basalt showed greater rates of Fe(III)-reduction at increasing soil moisture levels than granitic soils. Increases in Fe(III) reduction, however, were only associated with elevated rates of C mineralization in one basalt soil. Known Fe(III)-reducing taxa were present in all samples but neither the relative abundance nor richness of Fe(III)-reducers corresponded with measured rates of Fe(III) reduction. Under reducing conditions, Fe(III)-reduction was only coupled to C mineralization in the soil with the greatest amount of Fe-oxide bound C. However, Fe-oxide -bound C was below theoretical limits for C sorption onto Fe-oxides and not detectable in all soils. Overall, our results suggest that "what's there" in terms of soil chemistry may be a more important driver of C mineralization coupled to Fe(III) reduction than "who's there" in the microbial community.

Plain Language Summary The ability of soils to sequester and store carbon may depend, in large part, on associations between soil minerals and carbon molecules. Iron is associated with some of the oldest and most persistent soil carbon. However, in saturated soils microbial utilization of iron can lead to the loss of soil carbon. In this study, we explored how microbial utilization of iron under different soil moisture levels impacts rates of soil carbon loss and whether geologic differences in parent material or microbial community composition explain patterns between sites. To test this, we incubated soils from basalt and granitic parent material at different levels of soil moisture and tested rates of iron utilization and carbon decomposition. Differences in parent material impacted microbial utilization of iron but increases in iron utilization were only coupled to soil carbon decomposition in one soil. Iron reducing bacteria were present in all soils, regardless of rates of iron utilization, and differences in microbial community composition did not impact rates of iron utilization or soil carbon decomposition. Overall, our results suggest that site-specific soil chemistry may impact iron-carbon interactions more than microbial community composition or parent material.

1. Introduction

Iron-carbon (Fe-C) interactions impact long-term soil C stability, exerting both stabilizing and destabilizing influences depending on edaphic conditions. Under aerobic conditions, complex interactions among Fe-oxides, clay minerals, and organic matter may lead to long-term stabilization and physicochemical protection from microbial degradation (Barbera et al., 2008; Saidy et al., 2012; Wagai & Mayer, 2007; Wiseman & Pü, 2006). Poorly crystalline and short range order Fe-oxides, in particular, have high specific surface area that facilitate stabilization via sorption, coprecipitation, and/or occlusion processes and are associated with some of the most persistent terrestrial C (Hall & Huang, 2017; Torn et al., 1997).

Supervision: Benjamin W. Sullivan
Visualization: Cody C. Reed, Benjamin W. Sullivan
Writing – original draft: Cody C. Reed, Sarrah M. Dunham-Cheatham
Writing – review & editing: Cody C. Reed, Sarrah M. Dunham-Cheatham, Sarah C. Castle, David C. Vuono, Benjamin W. Sullivan

Under reducing conditions, dissimilatory reduction of Fe(III) minerals by microbes can destabilize Fe-C associations and may contribute substantially to soil C mineralization (Canfield et al., 1993; Lovley & Phillips, 1988; Roden & Wetzel, 1996, 2002). Amorphous and short range order Fe phases are particularly susceptible to redox effects and the dissolution of solid-phase Fe can further destabilizes Fe-C bonds, releasing mineral-associated C for microbial decomposition (Anthony & Silver, 2020; Huang & Hall, 2017; Lovley, 1987; Pan et al., 2016). While crystalline forms of Fe(III) tend to dominate in soils and sediments (Roden & Urrutia, 2002), frequent wet-dry periods common in humid and wetland soils may increase the fraction of amorphous and poorly crystalline Fe as repeated oxidation-reduction reactions limit formation of stable crystalline Fe(III)-oxides (Lovley & Phillips, 1987). Iron-reducing bacteria can also utilize humic substances to shuttle electrons to extracellular Fe(III)-oxides, enhancing rates of Fe(III) reduction and C mineralization in C-rich soils (Kappler et al., 2004; Lovley et al., 1996). In wetland soils, it is estimated that 35%–60% of carbon dioxide (CO_2) production may be attributed to decomposition of organic C coupled with dissimilatory Fe(III)-reduction (Lovley, 1987).

Montane meadows are mineral soil wetlands dominated by emergent vegetation sustained by shallow groundwater tables and periods of saturated soil conditions that extend into the growing season (Chambers & Miller, 2011; Wood, 1975). In the Sierra Nevada mountain range of California, Mediterranean climate patterns result in relatively short hydroperiods and seasonal fluctuations in depth to groundwater in meadows (Loheide et al., 2008; Loheide & Gorelick, 2007). This dynamic hydrology creates fluctuating redox conditions that allow Fe to be recycled as an electron acceptor through biotic and abiotic oxidation (Kaplan et al., 2016; Knorr et al., 2009; Yu & Kuzyakov, 2021), with potential implications for soil C cycling (Wang H. et al., 2019; Wang Y. et al., 2017). High rates of soil CO_2 efflux under saturated soil conditions in Sierra Nevada meadows (Reed et al., 2021) suggest that soil microbial communities may utilize alternate electron acceptors to decompose organic matter during periods when oxygen is limited and heterotrophic respiration should be suppressed. Simultaneous low rates of methanogenesis in these ecosystems (Reed et al., 2021) also raise the possibility that methane production may be suppressed by the reduction of alternative electron acceptors, including Fe(III)-oxides, under reducing conditions (Roden & Wetzel, 1996).

Meadows are hotspots of soil C in mountain regions (Norton et al., 2011, 2014; Reed et al., 2021) but have also long been focal points of human activity (Hughes, 1934; Hunsaker et al., 2015). Anthropogenic disturbance in meadows can result in disconnected floodplain hydrology, aerobic soil conditions, and loss of soil C (Norton et al., 2014; Reed et al., 2021). Restoration of floodplain hydrology has recently been proposed as an approach for increasing soil C sequestration, in addition to regenerating wildlife habitat and improving downstream water quality (National Fish and Wildlife Foundation, 2010). Recent studies suggest that restoration of floodplain hydrology in montane meadows may result in substantial belowground C gains (93–452 g C m^{-2} y^{-1}; Morra et al., 2023; Reed et al., 2022). However, these results are limited in geographic scope and soil forming factors. Differences in parent material that lead to variation in soil chemistry, particularly Fe- and Al-oxides, may interact with increasing reducing conditions and labile C inputs to influence the stabilization, destabilization, and mineralization of soil C following restoration (Coward et al., 2018; Kramer & Chadwick, 2018; McNicol & Silver, 2014). Specifically, by increasing the duration of anerobic soil conditions, restoration of floodplain hydrology may increase rates of C mineralization coupled to Fe(III) reduction that could attenuate C gains.

In this study, we explored the impact of inundation of meadow soils derived from parent materials with different soil chemistries (basalt or granite) on rates of dissimilatory microbial reduction of Fe(III). We hypothesized that rates Fe(III) reduction would increase with increasing levels of soil moisture and that Fe(III) reduction under these conditions would be linked to C mineralization as diffusion-limited oxygen concentrations should trigger the utilization of alternate electron acceptors (e.g., Fe) by native microbial communities. We also expected rates of Fe(III) reduction to be highest in soils derived from Fe-rich, basalt parent material. Finally, we hypothesized that differences in microbial community composition would explain discrepancies between soils with the same parent material.

2. Materials and Methods

2.1. Soil Description and Characterization

We conducted this study with soil collected from four montane meadows in the Sierra Nevada. Two meadows had soils derived from granite parent material while two meadows had soils derived from basalt parent material. The

Table 1
Climate and Soil Characteristics for Each of the Four Meadow Soils Used in This Study

Site	Latitude, longitude	Parent material	Elevation (m)	MAT (°C)	MAP (mm)	Soil
Benwood (G1)	38.8023 N, 120.0270 W	Granite	2,451	5.3	1,288.5	Mixed, fridid Dystric Xeropsamment
Star (G2)	38.8836 N, 119.9117 W	Granite	2,671	4.3	863.6	Oxyaquic Cryorthents-Aquic Xerorthent
Coyote (B1)	40.1106 N, 120.4203 W	Basalt	1,699	7.9	551.4	Loamy-skeletal, mixed Typic Cryumbrepts- Haplaquoll
East Creek (B2)	40.2378 N, 120.9131 W	Basalt	1,560	8.3	832.4	Fine-loamy, mixed, superactive, mesic Cumulic Endoaquoll

two granitic meadows, Benwood (G1) and Star (G2), were located on the south shore of Lake Tahoe in the Tahoe National Forest, CA. One basalt meadow, Coyote (B1), was located on the eastern side of the Plumas National Forest, CA. The second basalt meadow, East Creek (B2), was located on private land at the northern extent of the Sierra Nevada. The climate in all meadows is characterized as Mediterranean with warm, dry summers and cool, wet winters. Thirty-year averaged mean annual precipitation ranged from 551 to 1,288 mm and mean annual temperature from 4.3 to 8.3°C (PRISM Climate Group, 2010). Elevations ranged from 1,560 to 2,671 m asl (Table 1).

Within each meadow, soils were sampled to a depth of 50 cm at four randomly chosen points with at least 50 m between sampling locations. Within 24 h of collection, soils were sieved to remove the >2 mm fraction and air-dried at 21°C in a fume hood to expedite drying and minimize C transformations and losses due to microbial respiration. Replicates (n = 4) from each meadow were bulked and homogenized once air-dried and stored in brown paper bags (up to 1 month). Bulked soils were used for all experiments and analyses.

Two pools of C were quantified for each meadow soil: total solid-phase C and Fe oxide-bound organic C. Total solid-phase C and nitrogen (N) concentrations of replicate (n = 4 per meadow) pulverized soil aliquots were quantified using an elemental analyzer (EA; Costech 4010, Costech Analytical Technologies Inc., Valencia, CA, USA). We determined Fe oxide-bound C concentrations according to the acidified hydroxylamine hydrochloride (HH) method described in Chao and Zhou (1983). Briefly, replicate 0.1 g soil aliquots (n = 4 per meadow) were weighed into 50 mL centrifuge tubes. Two aliquots received 25 mL of reducing reagent (0.25 M HH plus 0.25 M HCl) and two aliquots received 25 mL of control reagent (0.75 M NaCl). All suspensions were heated in a 50°C water bath for 60 min, then centrifuged at 4,696 g_0 for 10 min, and the supernatants decanted into clean 50 mL centrifuge tube. The pellets were washed three times with 10 mL of Type 1 water (18 MΩ*cm) water, vortexed, centrifuged (5,000 rpm, 10 min) and the supernatant was decanted. The washed pellets were oven-dried at 60°C for 48 h and the C concentration measured using the Costech 4010. We repeated this process three times and used the mean of the control and HH-reduced values (n = 6). We calculated the Fe oxide-bound organic C concentration as the difference between the total C concentrations of control and HH-reduced soils. The supernatants were also analyzed using the ferrozine method (Stookey, 1970) to quantify the HH-extractable Fe concentration, used as a proxy for microbially-reducible Fe phases (Lovley & Phillips, 1987). The C:Fe molar ratio was calculated as the ratio of the molar mass of Fe oxide-bound C to the molar mass of HH-extractable Fe (Jeewani et al., 2021).

We used a 0.5 M hydrochloric acid (HCl) extraction method to quantify poorly crystalline, weak acid-extractable short range order Fe-oxides (Claff et al., 2010; Hall et al., 2016; Sidhu et al., 1981). Briefly, soil aliquots were reacted with weak hydrochloric acid (0.5 M HCl) at a soil:acid ratio of 1.00:1.25 for 24 h. The soil slurries were centrifuged (5,000 rpm for 10 min) and the Fe(II) concentration of the supernatant was quantified using the ferrozine method. We quantified the total extractable Fe content of the supernatant using the ferrozine assay with added excess HH to reduce aqueous Fe(III) to Fe(II).

2.2. Incubation Experiment

To determine the effect of soil moisture on C mineralization and Fe(III) reduction, we incubated soil from each of the four meadows under a range of soil moisture conditions. Prior to incubation, we determined the water holding capacity (WHC) of each soil based on the method described in Haubensak et al. (2002). A 10 g aliquot of

air-dried soil was wetted repeatedly with deionized water in a Büchner funnel on a wetted Whatman No. 1 filter paper for 24 h in an enclosed environment to prevent evaporative losses. We allowed the water to drain by gravity between wettings. To approximate soil field capacity, suction (−33 kPa) was applied to the gravity-drained soils until dripping stopped. The gravimetric water content of the soil at field capacity was then determined by drying the soil at 105°C to constant mass. We calculated the 100% WHC condition of the soil as the mass of water retained at field capacity divided by the oven-dried soil mass, multiplied by 100%.

Microcosms were constructed by adding 8 g of air-dried soil into uncapped 15 mL centrifuge tubes placed inside 250 mL media bottles. Each jar was fitted with a gas-tight lid containing a rubber septum to allow for gas sampling and contained 20 mL deionized water to maintain humidity within the jar and prevent evaporative loss from the soil. Deionized water was added to the soil in each tube to achieve a 45%, 60%, 75%, 90%, 115, 160%, or 200% WHC. Four replicates of each WHC were constructed for each meadow soil. To simulate slow wetting conditions most likely to be experienced in situ, the soils were incrementally wetted over a 4-day period by adding one fourth of the total water needed every 24 h until the target WHC was achieved. The incubation began on the first day of water addition.

We measured C mineralization over time by sampling headspace CO_2 concentrations in each jar on days 0, 1, 2, 3, 4, 7, 9, 11, and 14 of the incubation. Carbon dioxide concentrations were measured by removing 100 µL of headspace from each jar with a gastight syringe and needle assembly (Hamilton Company, Reno, Nevada, USA) and directly injecting the sample into an infrared gas analyzer (LI-8100, LI-COR Biosciences, Lincoln, Nebraska, USA). After each CO_2 measurement, the headspace was refreshed by flushing the jar with pressurized ambient atmosphere for 10 s before recapping the jar. Replicate ($n = 4$) soil-free control jars were used to quantify the concentration of ambient CO_2 in the jars after each flush. The mean value of the control jars was subtracted from the CO_2 concentration in each incubation jar to determine the amount of CO_2 evolved from the soil. Cumulative CO_2 production was calculated as the sum of CO_2 concentrations at each sampling time point per jar.

At the end of the 15-day incubation, we quantified the amount of Fe(III) reduction in each soil aliquot. Working inside an anaerobic chamber to prevent oxidation of Fe(II), we brought the water volume in each tube to 10 mL by adding N_2-sparged deionized water and dilute HCl to achieve a final HCl concentration of 0.5 M HCl. The acidified soil suspensions were vortexed until all soil particles were suspended and then left undisturbed in the anaerobic chamber. After 24 h, the suspensions were centrifuged (5,00 rpm, 10 min) and the Fe(II) and total Fe content of the supernatants were quantified using the ferrozine methods described above. Additionally, prior to acidification we measured the pH and redox potential (Eh) of the soils to verify that dissimilatory microbial Fe(III)-reduction was thermodynamically feasible in the samples most likely to be experiencing the maximum amount of Fe(III) reduction. Both pH and Eh were measured at 200% WHC using a YSI ORP probe (YSI Incorporated, Yellow Springs, Ohio, USA).

2.3. Microbe Swap

To assess the role of microbial community composition in mediating rates of dissimilatory microbial Fe(III)-reduction to CO_2, we performed a full factorial microbial swap experiment using the two basalt soils and measured rates of CO_2 production at 200% WHC over the course of a 15-day incubation. Soils were sterilized by autoclaving at 121°C for 1 h. Replicate microcosms ($n = 8$) for each sterilized soil were constructed as described above. While we recognize that complete sterilization of soils may not be possible, autoclaving has been shown to disrupt both cellular and extracellular biochemical processes associated with C cycling better than other techniques (Blankinship et al., 2014). To ensure no C mineralization was occurring in our sterilized samples, we incubated the sterilized soils and measured CO_2 production over 3 days prior to microbial inoculation.

Microbial communities were extracted from nonsterile soil from each site using an adapted method from Bottomley (1994). A 1:5 soil:sterile deionized water suspension was shaken for 30 min and filtered through a Whatman No. 40 filter into a sterile bottle. Small aliquots of the filtrates were immediately aseptically transferred to the sterile soil microcosms to achieve a final WHC of 200%. Microbial community inoculums extracted from each soil were added to sterilized soil from each site in a full factorial design with four replicates of each combination. Soil microcosms were incubated for 15 days, and headspace CO_2 concentrations were measured using the LI8100 on days 0, 3, 5, 7, 11 and 14. Jar headspaces were not flushed with ambient air following CO_2 measurements to prevent microbial contamination of the microcosms.

2.4. Illumina Bacterial 16S rRNA Gene Sequencing

We used high-throughput Illumina sequencing of 16S-V4 rRNA and ITS2 marker genes to determine microbial community composition. Amplicon sequencing was performed on each of the untreated soils (frozen on day 0 of the incubation) and replicates ($n = 3$) of the microbe swap samples (frozen at the end of the incubation). From each of the frozen soil samples, we extracted genomic DNA from 0.25 g subsamples following standard manufacturer's protocols for bulk DNA extractions with the Mo Bio PowerSoil™ kit (Mo Bio Laboratories, Inc., Carlsbad, USA). Genomic DNA samples were sent to the University of Minnesota Genomics Center for bacterial library preparation and sequencing. We used two-step dual-index PCR amplification of bacterial V4 regions of 16S rRNA gene in triplicate using KAPA HiFidelity Hot Start Polymerase (Gohl, MacLean, et al., 2016; Gohl, Vangay, et al., 2016). The first PCR-amplification of 16S-V4 was achieved using the universal bacterial primer set, 515F and 806R. A second PCR-amplification was used to add forward and reverse indexing primers to 5 µl of 1:100 PCR product from the first round of PCR. For all amplicon sequences, pooled, size-selected samples were denatured with NaOH, diluted to 8 pM in Illumina's HT1 buffer, spiked with 20% PhiX, and heat denatured at 96°C for 2 min immediately prior to loading. A MiSeq 600 cycle v3 kit was used to sequence samples on an Illumina MiSeq machine.

For bacteria, OTU picking and taxonomic assignment were achieved using the Mothur SOP pipeline (Schloss et al., 2009) and the 97% greengenes database (The Greengenes Database Consortium: http://greengenes.secondgenome.com). Singletons represented only once across the data set were removed prior to OTU clustering. OTUs representative of mitochondria, chloroplasts, and sequences of unknown origin were removed prior to rarefaction. To equalize across samples of varying sequence numbers, samples were rarefied to depth 7300 sequences per sample. Post-pipeline calculations were done using QIIME 1.9 (Caporaso et al., 2010) and R v.3.1.1 (R Core Team, 2017).

A total of 116,800 high quality 16S V4 bacterial sequences were recovered from 17 soil mesocosm samples. Among all rarefied bacterial samples, we found a total of 5,652 database referenced OTUs. Sequences have been uploaded to the NCBI Sequence Read Archive public repository under the BioProject number PRJNA901460.

We then built a custom database of known Fe(III)-reducers to compare against the 16S sequences from our samples. As there is no universal gene for Fe(III) reduction, we identified 40 known Fe(III)-reducers from literature and downloaded 16S rRNA sequences for each from the SILVA database (https://www.arb-silva.de). A custom BLAST database was developed for the known Fe(III)-reducers and a targeted BLAST run against the rarefied 16S sequences for each sample using the NCBI Genome Workbench (https://www.ncbi.nlm.nih.gov/tools/gbench/). Of the 40 known Fe-reducers in the database, 12 were identified in our samples (see Figure S1).

2.5. Statistical Analysis

All data were analyzed using R statistical software versions 3.1.1 and 4.0.3 (R Core Team, 2017, 2020). We used Kruskal-Wallis one-way analysis of variance to test differences in Fe(III) reduction and C mineralization among the four soils and identified post-hoc pairwise differences using Conover-Iman tests. Statistical significance was set a priori to $\alpha = 0.05$.

Metrics of alpha diversity, based on OTU richness and Shannon H' Index, were explored using the "vegan" package in R (Oksanen et al., 2018). Beta diversity was assessed with Hellinger abundance transformed OTU-based Bray-Curtis distances (BC-OTU) using principal coordinates analyses in the R package "vegan." Significant differences in community composition among sites and treatments were tested using permutational analysis of variance on distance matrices (PERMANOVA; Anderson, 2001) with the Adonis function in the "vegan" package.

3. Results and Discussion

Soil C concentration ranged from 27.97 ± 0.94 to 42.85 ± 7.71 mg C g^{-1} and was higher in the granitic soils than the basalt soils (Table 2). Soil N concentration ranged from 1.70 ± 0.05 to 3.33 ± 0.23 mg N g^{-1} and was highest in the granitic soil G1. The C:N ranged from 12.85 (G1) to 16.43 (B1). Fe-oxide bound C constituted ~4% of total soil C in the basalt soils (Table 2). In the granitic soils, we measured less C in the HH-extracted samples than the controls, which we interpreted as undetectable levels of Fe-oxide bound C. Short range order Fe

Table 2
Chemical Properties of Soils Prior to Incubation

Parameter	Unit	Benwood (G1)	Star (G2)	Coyote (B1)	East Creek (B2)
Total C	mg C/g soil	42.85 ± 7.71	32.27 ± 2.90	27.97 ± 0.94	28.32 ± 0.37
Total N	mg N/g soil	3.33 ± 0.23	2.02 ± 0.21	1.7 ± 0.05	2.04 ± 0.03
C:N		12.85	16.01	16.43	13.85
Fe-oxide bound C	mg C/g soil	ND	ND	1.03	1.15
	% of Total C	ND	ND	3.69	4.07
C:Fe molar ratio [a]		ND	ND	0.64	0.42
Reductive Dissolution Extractable Fe [a]	mg Fe/g soil	6.67 ± 0.89	4.42 ± 0.46	7.47 ± 0.75	12.78 ± 0.84
Acid Extractable Fe [b]	mg Fe/g soil	1.75 ± 0.02	1.16 ± 0.15	0.5 ± 0.32	1.72 ± 0.09

Note. ND = none detected. Measurements include total carbon (C) concentration, total nitrogen (N) concentration, ratio of C:N, concentration Fe-oxide bound C, molar ratio of Fe-oxide bound C to microbially available Fe (C:Fe), reductive dissolution extractable and acid extractable Fe, and concentrations of acid extractable Fe(II).
[a]Using hydroxylamine hydrochloride extraction method, a proxy for microbially-reducible Fe phases. [b]Using hydrochloric acid extraction method, a proxy for SRO (short-range order) Fe phases.

phases ranged from 0.5 to 1.75 mg Fe g^{-1} with the lowest concentration measured in the basalt soil B1 (Table 2). Microbially-reducible Fe concentrations ranged from 4.42 to 12.78 mg Fe g^{-1} with the lowest concentration measured in G2 and the highest in B2 (Table 2).

3.1. Fe(III)-Reduction

The fraction of total Fe reduced to Fe(II) over the course of the incubation was small (<15%) in all soils at 45%, 60%, 75%, and 90% WHC. Oxidation of Fe(II) was also present at these WHC in all soils except B2. At 115% WHC, the fraction of Fe as Fe(II) increased in both basalt soils but did not increase in either of the granitic soils (Figures 1a and 1b). This finding supports our hypothesis that differences in parent material are associated with differential rates of Fe(III) reduction, even though concentrations of Fe and C did not vary consistently by soil type. At 200% WHC, production of Fe(II) increased in one granitic soil (G1) but remained low in the other (G2; Figure 1b). At 200% WHC, <1% of Fe was reduced to Fe(II) in G2, whereas up to 70% of Fe was reduced to Fe(II) in the other soils (G1: 35.17 ± 5.26%, B1: 44.92 ± 8.66%, B2: 70.26 ± 13.98%; Figures 1a and 1b). Overall, our hypothesis that Fe(III) reduction would increase with increasing soil moisture was supported in the basalt soils but not consistently in the granitic soils.

3.2. CO_2 Production

Cumulative CO_2 production displayed the expected negative parabolic relationship with soil moisture in one granitic soil (G1, peak at 115% WHC) and one basalt soil (B1, peak at 90% WHC; Figures 1c and 1d). Peak rates of C mineralization in both soils occurred at higher levels of soil moisture than typically observed for upland and peat soils (Wen et al., 2019). Carbon mineralization in the other granitic soil (G2) increased with increasing soil moisture until 90% WHC and leveled off, remaining relatively high at 200% WHC despite a lack of Fe(II)-production (Figure 1d). Mean cumulative CO_2 production, normalized by soil C concentration, was highest in B2 at all soil moisture levels and reached its maximum value at 200% WHC. Cumulative CO_2 production was significantly different between the two basalt soils at 45%, 90%, 110%, and 200% WHC (Figure 1c) whereas it was only significantly different between the two granitic soils at 45% WHC (Figure 1d).

Assuming all Fe(II) produced over the course of the incubation was coupled with C mineralization, dissimilatory reduction of Fe(III) in the three soils where Fe(II) production occurred accounted for 25% (B1), 50% (B2), and 89% (G1) of CO_2 production at 200% WHC (using a 4:1 M ratio of C mineralization to Fe(III) reduction; Roden & Wetzel, 1996). The estimated contributions of Fe(III) reduction to CO_2 production for the basalt soils are in line with values reported for wetlands (Lovley, 1987) and tropical forests (Dubinsky et al., 2010). In the granitic soil (G1), dissimilatory reduction of Fe(III) could potentially explain almost all of the CO_2 production at 200% WHC. However, it is important to note that CO_2 production was lowest in G1 at 200% WHC and there was no Fe(II) production at 160% WHC.

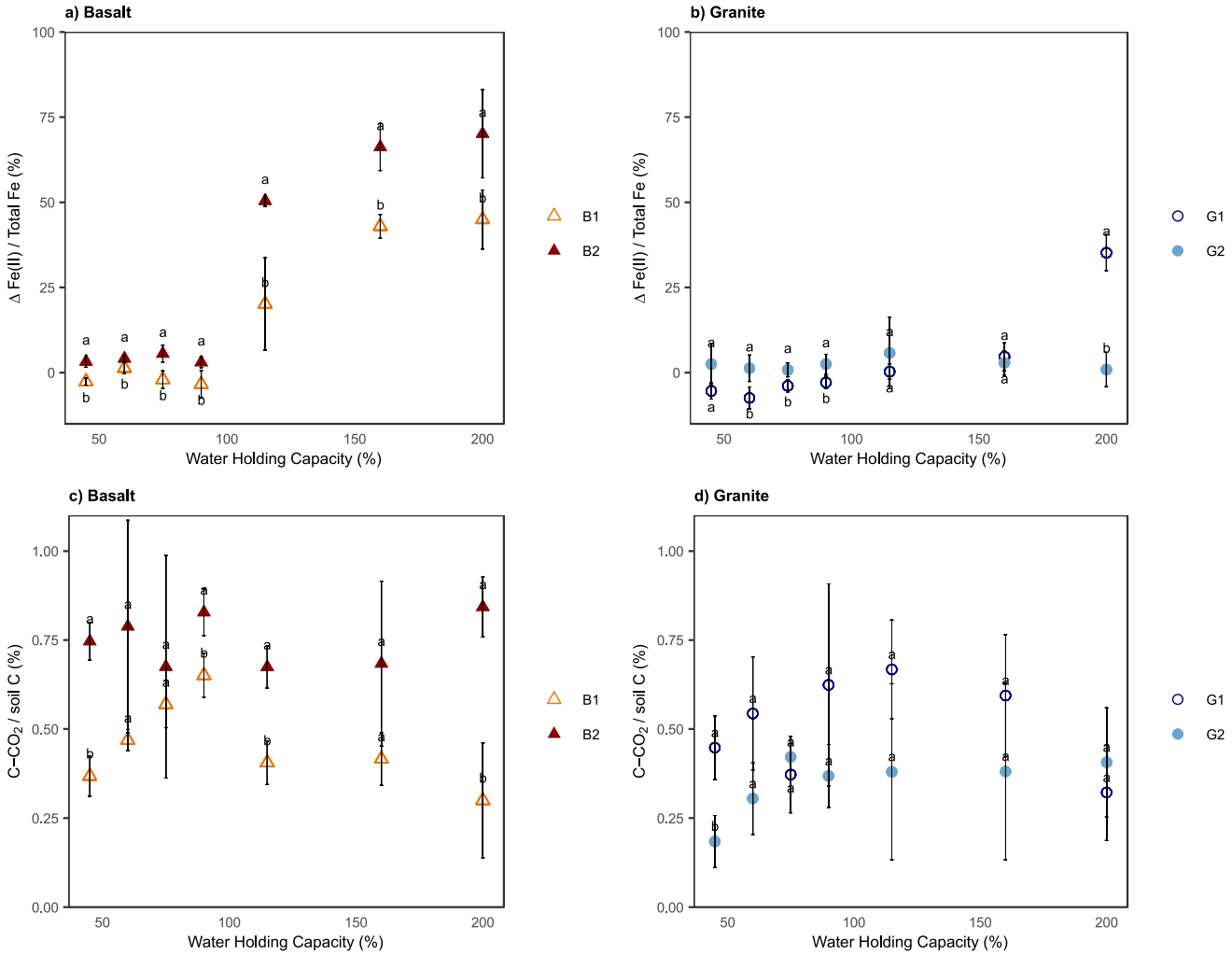

Figure 1. Relationships between soil water holding capacity, Fe(III) reduction and CO_2 production. Fe(III) reduction, measured as the increase in Fe(II) concentration relative to total Fe, for basalt (a) and granitic (b) soils. Rates of CO_2 emission normalized by soil carbon concentration, for basalt (c) and granitic (d) soils. Results show cumulative CO_2 production and Fe(III) reduction over the course of the 15-d incubation. Letters denote significant differences among soils for each parent material.

Overall, Fe(II) production at higher soil moisture levels was only coupled with high cumulative CO_2 production, as we had originally hypothesized, in one soil (B2). Reduction of Fe(III) at higher soil moisture levels in G1 and B1 was not associated with increases in C mineralization. These findings highlight the valuable context that can be gained from studying reactions across a range of soil moisture levels. They also raise questions about the contribution of other electron acceptors and microbial pathways to C fluxes in montane meadows. The results of G1, in particular, may be better explained by dissimilatory Fe(III)-reduction coupled to the oxidation of ammonium, a process known as Feammox (Clément et al., 2005). In addition to Fe(III) reduction that was not coupled to increasing C mineralization, this soil had the highest total N concentration and lowest C:N of any of the four sites. Feammox is an important pathway for N loss in terrestrial ecosystems including forests (Yang et al., 2012) and wetlands (Clément et al., 2005; Shrestha et al., 2009) but has not yet been studied in montane meadows.

Abiotic oxidation of Fe(II) by reactive oxygen species via Fenton and Fenton-like reactions could be another potential explanation for the low rates of Fe(II) production in the grantic soils under elevation soil moisture levels despite the presence of Fe(III)-reducing taxa (Chen et al., 2020; Hall & Silver, 2013; Merino et al., 2020). Iron(II) produced through dissimilatory microbial reduction may have been oxidized to Fe(III) by hydrogen peroxide or other reactive oxygen species. However, Fenton reactions also produce hydroxyl radicals that are powerful oxidants of soil organic matter. If abiotic Fe(II) oxidation were limiting rates of net Fe(II) production, we would still expect to see elevated rates of C mineralization under higher soil moisture levels. It seems possible, therefore

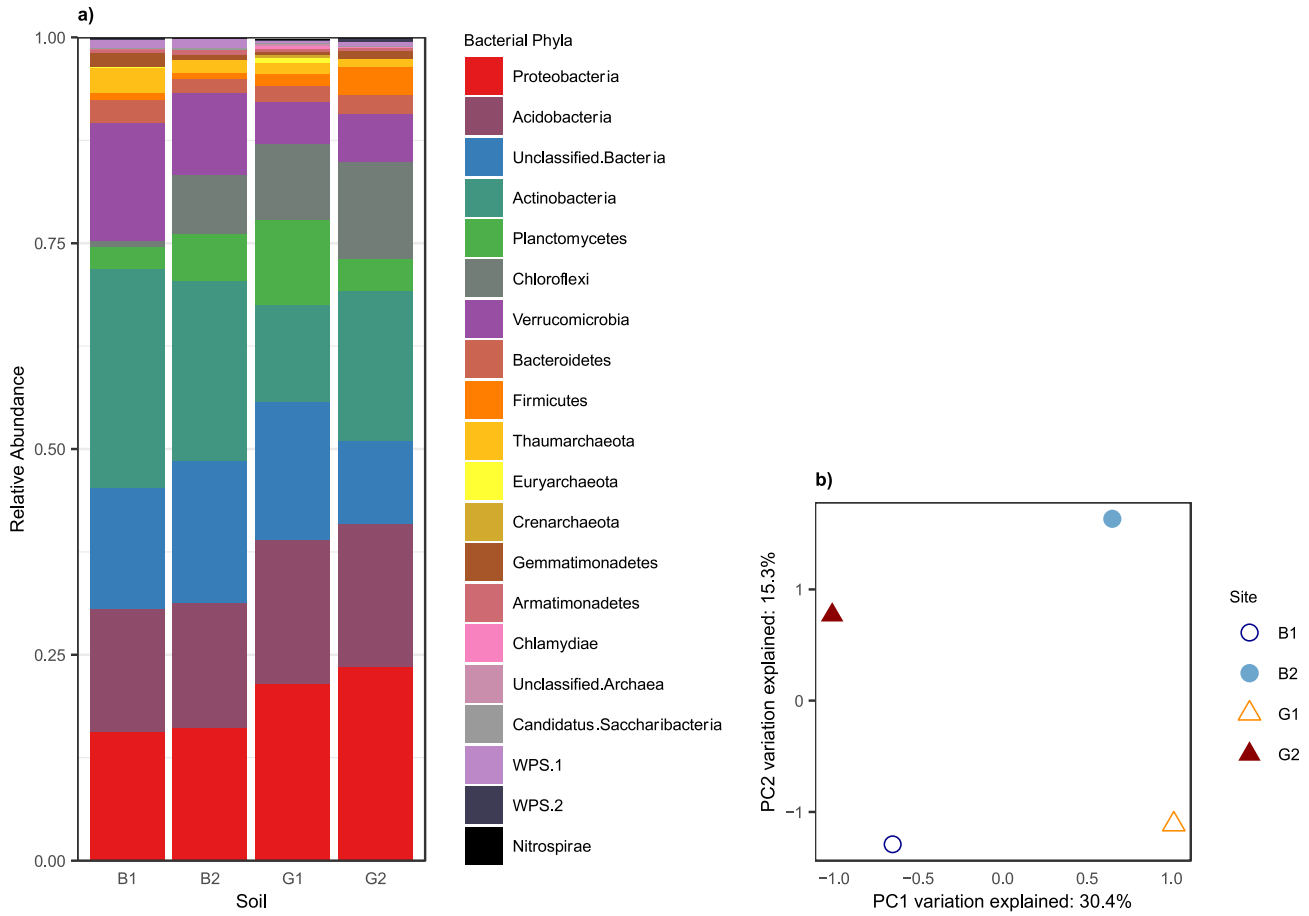

Figure 2. Relative abundance of bacteria at the phylum level in each of the native soils (a). Bacterial community composition was not similar in any of the four native soils (b).

that Fenton reactions may have contributed to the sustained rates of C mineralization with increasing soil moisture observed in G2 but are unlikely to explain the patterns observed in G1 (Figure 1).

3.3. Microbial Community Composition

Bacteria communities at the phyla level were dominated by *Proteobacteria*, *Acidobacteria*, and *Actinobacteria* in all soils but community composition at the taxa level was not similar in any of the sites (Figure 2). Eleven taxa of known Fe(III)-reducers were recovered from the native soils and six taxa (*Rhodoferax ferrireducens, Geobacter metallireducens, Clostridium beijerinckii, Bacillus infernus, Desulfosporosinus meridiei, Anaeromyxobacter dehalogenans*) were present in all soils (Figure 3). No Fe(III)-reducing archaea were identified nor were any taxa associated with the model Fe(III)-reducer *Shewanella*.

Five of the Fe(III)-reducing taxa identified are additionally known to perform Feammox (Yao et al., 2020; Zhu et al., 2022). One of these five taxa, *Geothrix fermentans*, was only present in the granitic soil, G1, with high rates of Fe(III) reduction and low rates of cumulative C mineralization at 200% WHC.

The highest relative abundance of Fe(III)-reducers was identified in the soil with the lowest rate of Fe(III) reduction, G2 (Figure 3). The presence of taxa capable of dissimilatory Fe(III)-reduction in this soil despite low levels of Fe(II) production may be explained by the ability of many Fe(III)-reducing bacteria to use alternate electron acceptors including nitrate, manganese (IV), and sulfate (He & Sanford, 2003; Lovley & Holmes, 2004; Lovley & Phillips, 1988). However, lower rates of C mineralization across all water contents relative to the other soils also point to decreased levels of microbial activity in G2. The greatest richness and diversity of known

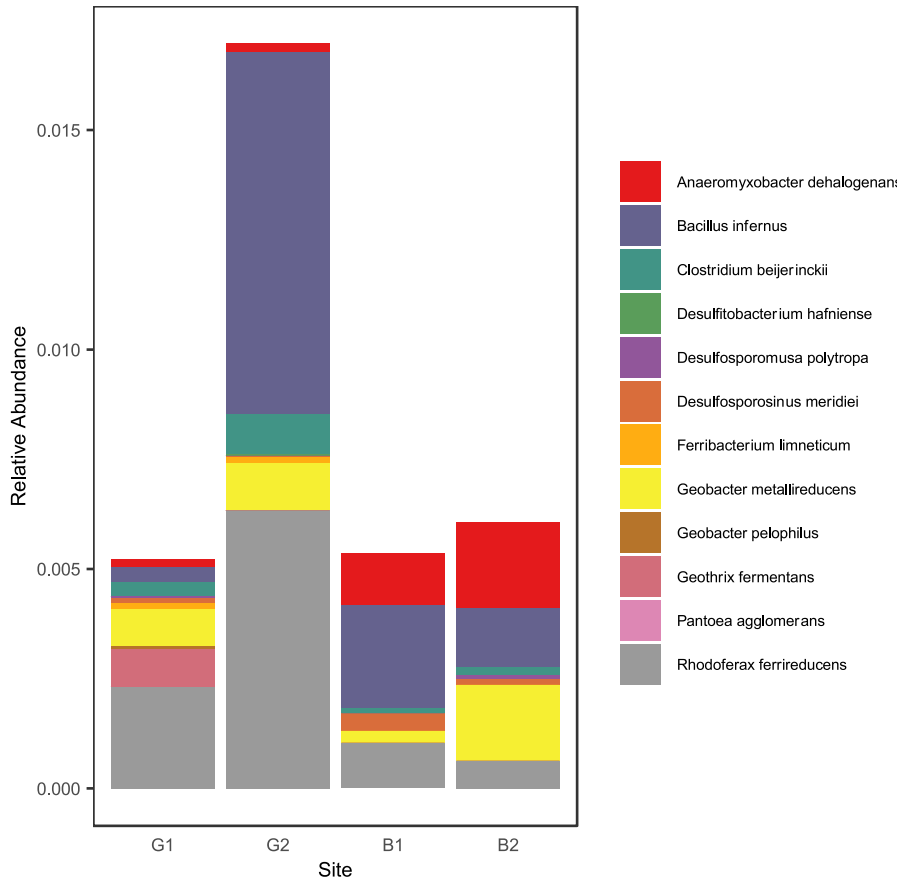

Figure 3. Relative abundance of known Fe(III)-reducing bacteria recovered from each of the native soils.

Fe(III)-reducers was found in G1, which had Fe(III) reduction at 200% WHC without commensurate increases in CO_2 production (Table 3), further supporting the metabolic flexibility of many known Fe(III)-reducers and suggesting the occurrence of alternate metabolic pathways in our samples.

Varying rates of Fe(III) reduction measured during the incubation, despite the ubiquity of Fe(III)-reducing taxa in our samples, highlight the challenges associated with assigning ecosystem function based on microbial community composition in native soils. These results may also point to the role of soil chemistry in regulating dissimilatory Fe(III)-reduction. Anthony and Silver (2020) found that higher concentrations of microbially-reducible Fe species were associated with soil C loss in reflooded wetland sites. Similarly, in our study, the highest concentration of microbially-reducible Fe was measured in the soil with increasing Fe(II) production and high rates of C mineralization at elevated soil moisture levels (B2; Table 2). In addition to Fe species, C substrate may shape microbial community composition and rates of Fe(III) reduction (Lentini et al., 2012). Limited, preliminary data suggest that the basalt soils may have had more aromatic C than the granitic soils in this experiment (data not shown). However, these results are preliminary, and we acknowledge that C chemistry does not necessarily equate to bioavailability. Future studies that involve isotopic labeling of C substrates are needed to determine the impact of C chemistry on dissimilatory Fe(III)-reduction in montane meadows.

Table 3
Richness and Alpha Diversity Fe(III)-Reducing Community Recovered From Native Soils

Soil	G1	G2	B1	B2
Richness (H_0)	10	8	6	7
Exp Shannon (H_1)	5.38	3.21	4.23	4.68

Note. Alpha diversity of Fe(III)-reducing communities was calculated using the Shannon Index to capture both richness and evenness of the community.

The low concentrations of Fe-oxide bound C may also be linked to the inconsistent relationship observed between Fe(III) reduction and C mineralization. In ecosystems with dynamic redox conditions, Fe-bound C formed during periods of aerobic soil conditions may be completely mineralized during periods of anoxia (Huang et al., 2020; Patzner et al., 2020, 2022). The granitic soils were from higher elevation sites with more soil moisture at the

time of sampling (data not shown). Less C complexed with Fe at the start of the incubation may have contributed to the lower rates of dissimilatory Fe(III)-reduction observed in these soils.

Even at the site with the highest concentration of Fe-oxide bound C (B2), concentrations were well below theoretical limits for organic C sorption onto Fe-oxides (Kaiser et al., 1997; Wagai & Mayer, 2007). Further, the fraction of total C complexed with Fe was lower than values reported for agricultural soils (Wan et al., 2019), wetlands (Duan et al., 2020; Shields et al., 2016) and mangroves (Dicen et al., 2019). These results may be due in part to the timing of soil collection and the seasonal nature of Fe-oxide bound C in these ecosystems. However, they also raise the possibility that Fe-organic matter complexes may play a smaller role in the long-term stabilization of C in montane meadows than other ecosystems.

Recent research suggests that aluminum may be more important than Fe for long-term C stabilization in ecosystems with dynamic redox conditions (Anthony & Silver, 2020; Kramer & Chadwick, 2018). Future research should consider the type of both Fe- and Al-organic matter complexes present in soils and collect samples at multiple points throughout the year to determine the impact of changing redox conditions on C stabilization and mineralization.

3.4. Microbe Swap

We were intrigued by the fact that Fe(III) reduction appeared to be coupled to CO_2 production in one basalt soil (B2) but not the other (B1). This divergent response between the basalt soils compelled us to explore the role of microbial community composition in mediating rates of C mineralization via dissimilatory microbial reduction of Fe(III). As we expected, the composition of known Fe(III)-reducers was substantially different in all of the microbe-swap soils at the end of the incubation relative to the native soils (Figure 4a). A priori, we acknowledged that the extraction and inoculation process would alter the microbial community composition but aimed for consistent alteration of both communities. *Pantoea agglomerans*, in particular, was present in all soils with inoculum extracted from B2 but not detected in any of the native soils. *Pantoea agglomerans* is a facultative anaerobic bacteria that can couple Fe(III) reduction with the oxidation of acetate or H_2 (Francis et al., 2000). Other taxa that were common in the native soils (e.g., *Aneromyxobacter dehalogenans, Bacilius infernus, Desulfosporosinus meridiei, Ferribacterium limneticum,* and *Rhodoferax ferrireducens*) were not detected or only detected in a few replicates of the microbe-swap soils. The relative abundance of Fe(III)-reducers was also one to two orders of magnitude higher in the microbe-swap soils than the native soils. It should be noted, that the DNA extraction of the microbe-swap soils was performed at the end of the 15-day incubation as opposed to the beginning of the incubation for the native soils. It is possible that changes in bacterial community composition occurred over the course of the incubation as a result of sustained reducing conditions. It is not uncommon in microbial communities for extremely rare taxa to replace dominant ones over the course of a few weeks (Fernández et al., 1999; Fernandez-Gonzalez et al., 2016), even if only a weak competitive advantage exists, and similar shifts toward bacterial communities enriched in taxa capable of Fe-cycling have been observed following prolonged anoxia (Bhattacharyya et al., 2018).

The microbial communities at the end of the incubation differed significantly by inoculum ($p < 0.01$, $F = 8.23$), not by soil ($p = 0.35$, $F = 1.28$; Figure 4b). However, rates of C mineralization over the course of the incubation were consistently higher in samples with B2 soils, regardless of inoculum source ($p < 0.01$, Figure 4c). Interestingly, while the molar ratios of Fe-oxide bound C to microbially available Fe (C:Fe) were suggestive of sorption interactions for both basalt soils (C:Fe < 1; Wagai & Mayer, 2007), the ratio was lowest for B2. This site also had the highest fraction of total C as Fe-oxide bound C (Table 2), suggesting a somewhat larger pools of readily-degradable C temporarily stabilized by weak sorptive interactions. Other studies have shown that biogeochemical flux rates appear to be coupled more to environmental factors than species assemblages and relatively insensitive to taxonomic changes within functional groups (Fernández et al., 1999; Louca et al., 2016, 2018; Nelson et al., 2016). Our results similarly suggest that microbial community composition may have less influence on biogeochemical processes than environmental or edaphic characteristics.

In other words, "what's there" in terms of soil chemistry appears be more important than "who's there" in the microbial community. Overall, our results highlight the complexity of biogeochemical cycles and the fact that just measuring rates of target chemical species may miss important processes. To more comprehensively determine the drivers, all potential electron acceptors and donors should be accounted for, and the activity of the microbial

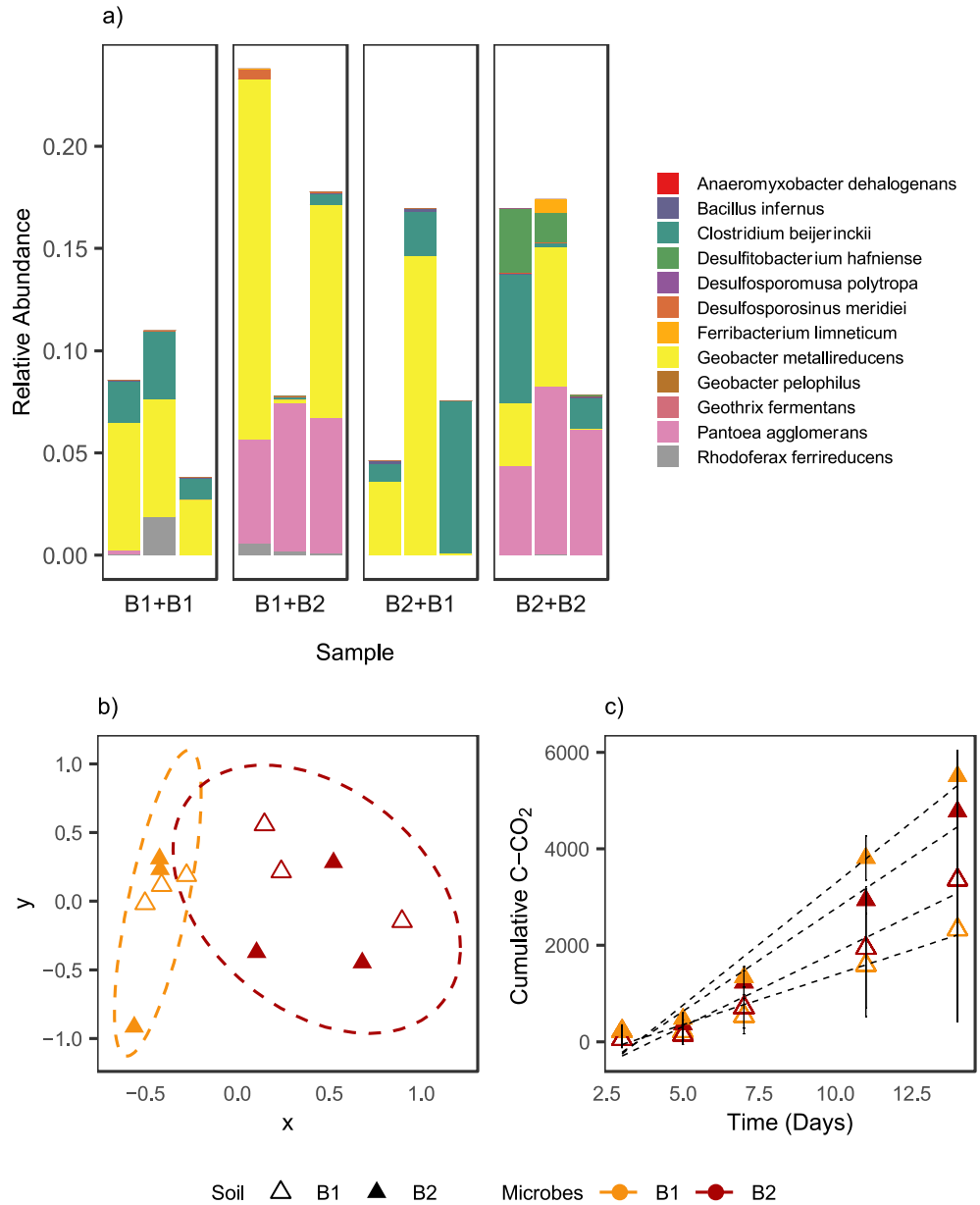

Figure 4. Relative abundance of known Fe(III)-reducing bacteria in each of the microbe-swap samples at the end of the 15-d incubation (a). Permutational multivariate analysis of variance (PERMANOVA) analysis of normalized multidimensional scaling (NMDS) revealed that microbial communities at the end of the incubations differed significantly by innoculum ($p < 0.01$, $F = 8.23$), but not by soil ($p = 0.35$, $F = 1.28$); (b) Despite differences in microbial community composition, cumulative CO_2 production over the course of the incubation was significantly higher ($p < 0.01$) in samples with B2 soils, regardless of inoculum.

community should be quantified. Further, changes in environmental conditions can alter both soil chemistry and microbial community response. Laboratory incubations or results from limited time points can provide valuable information on mechanistic responses but should be applied to ecosystems and models with caution.

4. Conclusion

Together, our results suggest that Fe(III) reduction may contribute to increased rates of C mineralization following restoration of floodplain hydrology in montane meadows but is not universally present under reducing conditions.

The occurrence of dissimilatory microbial Fe(III)-reduction may be more dependent on site-specific soil chemistry than parent material, making broad-scale generalizations tenuous. Interest in restoration and conservation of montane meadows and other wetland ecosystems has increased in recent years because of their disproportionate impact on regional C cycles (Norton et al., 2014; Reed et al., 2021) and potential to sequester large amounts of soil C (Reed et al., 2022). While our results suggest that dissimilatory Fe(III)-reduction may not be widespread under saturated soil conditions, they also raise questions about the impact of Fe to long-term stabilization of C in meadows. Greater understanding mineral-C interactions under changing redox conditions is needed to accurately predict the impacts of anthropogenic disturbance and restoration in montane meadows on greenhouse gas fluxes and regional C budgets.

Conflict of Interest

The authors declare no conflicts of interest relevant to this study.

Data Availability Statement

Data are available from Dryad at https://doi.org/10.5061/dryad.qjq2bvqkn. All 16s V-4 rRNA sequences are available at the NCBI Sequence Read Archive public repository under the BioProject no. PRJNA901460. All data were analyzed and figures made using R statistical software version 4.0.3 (R Core Team, 2020).

Acknowledgments
Cody C. Reed and Benjamin W. Sullivan were partially supported by the California Department of Fish and Wildlife (P149600200). Other funding came from University of Nevada, Reno startup support to Benjamin W. Sullivan.

References

Anderson, M. J. (2001). A new method for non-parametric multivariate analysis of variance. *Austral Ecology*, *26*(1), 32–46. https://doi.org/10.1111/j.1442-9993.2001.tb00081.x

Anthony, T. L., & Silver, W. L. (2020). Mineralogical associations with soil carbon in managed wetland soils. *Global Change Biology*, *26*(11), 6555–6567. https://doi.org/10.1111/gcb.15309

Barbera, V., Raimondi, S., Egli, M., & Plötze, M. (2008). The influence of weathering processes on labile and stable organic matter in Mediterranean volcanic soils. *Geoderma*, *143*(1–2), 191–205. https://doi.org/10.1016/j.geoderma.2007.11.002

Bhattacharyya, A., Campbell, A. N., Tfaily, M. M., Lin, Y., Kukkadapu, R. K., Silver, W. L., et al. (2018). Redox fluctuations control the coupled cycling of iron and carbon in tropical forest soils. *Environmental Science and Technology*, *52*, 14129–14139. https://doi.org/10.1021/acs.est.8b03408

Blankinship, J. C., Becerra, C. A., Schaeffer, S. M., & Schimel, J. P. (2014). Separating cellular metabolism from exoenzyme activity in soil organic matter decomposition. *Soil Biology and Biochemistry*, *71*, 68–75. https://doi.org/10.1016/j.soilbio.2014.01.010

Bottomley, P. J. (1994). Light microscopic methods for studying soil microorganisms. In R. W. Weaver, S. Angle, P. J. Bottomley, D. Bezdicek, S. Smith, A. Tabatabai, et al. (Eds.), *Methods of soil analysis Part 2: Microbiological and biochemical properties* (pp. 81–105). Soil Science Society of America.

Canfield, D. E., Thamdrup, B., & Hansen, J. W. (1993). The anaerobic degradation of organic matter in Danish coastal sediments: Iron reduction, manganese reduction, and sulfate reduction. *Geochimica et Cosmochimica Acta*, *57*(16), 3867–3883. https://doi.org/10.1016/0016-7037(93)90340-3

Caporaso, J. G., Kuczynski, J., Stombaugh, J., Bittinger, K., Bushman, F. D., Elizebeth, K. C., et al. (2010). QIIME allows analysis of high-throughput community sequencing data. *Nature Methods*, *7*(5), 1–4. https://doi.org/10.1038/nmeth.f.303.QIIME

Chambers, J. C., & Miller, J. R. (Eds.) (2011). *Geomorphology, hydrology, and ecology of great basin meadow complexes — implications for management and restoration (gen. Tech. Report. RMRS-GTR-258)*. U.S. Department of Agriculture, Forest Service, Rocky Mountain Research Station.

Chao, T. T., & Zhou, L. (1983). Extraction techniques for selective dissolution of amorphous iron oxides from soils and sediments. *Soil Science Society of America Journal*, *47*(2), 225–232. https://doi.org/10.2136/sssaj1983.03615995004700020010x

Chen, C., Hall, S. J., Coward, E., & Thompson, A. (2020). Iron-mediated organic matter decomposition in humid soils can counteract protection. *Nature Communications*, *11*(1), 1–13. https://doi.org/10.1038/s41467-020-16071-5

Claff, S. R., Sullivan, L. A., Burton, E. D., & Bush, R. T. (2010). A sequential extraction procedure for acid sulfate soils: Partitioning of iron. *Geoderma*, *155*(3–4), 224–230. https://doi.org/10.1016/j.geoderma.2009.12.002

Clément, J. C., Shrestha, J., Ehrenfeld, J. G., & Jaffé, P. R. (2005). Ammonium oxidation coupled to dissimilatory reduction of iron under anaerobic conditions in wetland soils. *Soil Biology and Biochemistry*, *37*(12), 2323–2328. https://doi.org/10.1016/j.soilbio.2005.03.027

Coward, E. K., Thompson, A., & Plante, A. F. (2018). Contrasting Fe speciation in two humid forest soils: Insight into organomineral associations in redox-active environments. *Geochimica et Cosmochimica Acta*, *238*, 68–84. https://doi.org/10.1016/j.gca.2018.07.007

Dicen, G. P., Navarrete, I. A., Rallos, R. V., Salmo, S. G., & Garcia, M. C. A. (2019). The role of reactive iron in long-term carbon sequestration in mangrove sediments. *Journal of Soils and Sediments*, *19*(1), 501–510. https://doi.org/10.1007/s11368-018-2051-y

Duan, X., Yu, X., Li, Z., Wang, Q., Liu, Z., & Zou, Y. (2020). Iron-bound organic carbon is conserved in the rhizosphere soil of freshwater wetlands. *Soil Biology and Biochemistry*, *149*, 107949. https://doi.org/10.1016/j.soilbio.2020.107949

Dubinsky, E. A., Silver, W. L., & Firestone, M. K. (2010). Tropical forest soil microbial communities couple iron and carbon biogeochemistry. *Ecology*, *91*(9), 2604–2612. https://doi.org/10.1890/09-1365.1

Fernández, A., Huang, S., Seston, S., Xing, J., Hickey, R., Criddle, C., & Tiedje, J. (1999). How stable is stable? Function versus community composition. *Applied and Environmental Microbiology*, *65*(8), 3697–3704. https://doi.org/10.1128/aem.65.8.3697-3704.1999

Fernandez-Gonzalez, N., Huber, J. A., & Vallino, J. J. (2016). Microbial communities are well adapted to disturbances in energy input. *mSystems*, *1*(5), e001177–16. https://doi.org/10.1128/msystems.00117-16

Francis, C. A., Obraztsova, A. Y., & Tebo, B. M. (2000). Dissimilatory metal reduction by the facultative anaerobe Pantoea agglomerans SP1. *Applied and Environmental Microbiology*, *66*(2), 543–548. https://doi.org/10.1128/AEM.66.2.543-548.2000

Gohl, D. M., MacLean, A., Hauge, A., Becker, A., Walek, D., & Beckman, K. B. (2016). An optimized protocol for high-throughput amplicon-based microbiome profiling. *Protocol Exchange*. https://doi.org/10.1038/protex.2016.030

Gohl, D. M., Vangay, P., Garbe, J., MacLean, A., Hauge, A., Becker, A., et al. (2016). Systematic improvement of amplicon marker gene methods for increased accuracy in microbiome studies. *Nature Biotechnology*, *34*(9), 942–949. https://doi.org/10.1038/nbt.3601

Hall, S. J., & Huang, W. (2017). Iron reduction: A mechanism for dynamic cycling of occluded cations in tropical forest soils? *Biogeochemistry*, *136*(1), 91–102. https://doi.org/10.1007/s10533-017-0383-0

Hall, S. J., & Silver, W. L. (2013). Iron oxidation stimulates organic matter decomposition in humid tropical forest soils. *Global Change Biology*, *19*(9), 2804–2813. https://doi.org/10.1111/gcb.12229

Hall, S. J., Silver, W. L., Timokhin, V. I., & Hammel, K. E. (2016). Iron addition to soil specifically stabilized lignin. *Soil Biology and Biochemistry*, *98*, 95–98. https://doi.org/10.1016/j.soilbio.2016.04.010

Haubensak, K. A., Hart, S. C., & Stark, J. M. (2002). Influences of chloroform exposure time and soil water content on C and N release in forest soils. *Soil Biology and Biochemistry*, *34*(11), 1549–1562. https://doi.org/10.1016/S0038-0717(02)00124-4

He, Q., & Sanford, R. A. (2003). Characterization of Fe(III) reduction by chlororespiring Anaeromxyobacter dehalogenans. *Applied and Environmental Microbiology*, *69*(5), 2712–2718. https://doi.org/10.1128/AEM.69.5.2712-2718.2003

Huang, W., & Hall, S. J. (2017). Elevated moisture stimulates carbon loss from mineral soils by releasing protected organic matter. *Nature Communications*, *8*(1), 1774. https://doi.org/10.1038/s41467-017-01998-z

Huang, W., Ye, C., Hockaday, W. C., & Hall, S. J. (2020). Trade-offs in soil carbon protection mechanisms under aerobic and anaerobic conditions. *Global Change Biology*, *26*(6), 3726–3737. https://doi.org/10.1111/gcb.15100

Hughes, J. E. (1934). *Erosion control progress report*. U.S. Department of Agriculture, Forest Serivce.

Hunsaker, C., Swanson, S., McMahon, A., Viers, J., & Hill, B. (2015). *Effects of meadow erosion and restoration on groundwater storage and baseflow in national forests in the Sierra Nevada* (Vol. 1–59). USDA Forest Service.

Jeewani, P. H., Ling, L., Fu, Y., Van Zwieten, L., Zhu, Z., Ge, T., et al. (2021). The stoichiometric C-Fe ratio regulates glucose mineralization and stabilization via microbial processes. *Geoderma*, *383*, 114769. https://doi.org/10.1016/j.geoderma.2020.114769

Kaiser, K., Guggenberger, G., Haumaier, L., & Zech, W. (1997). Dissolved organic matter sorption on subsoils and minerals studied by 13C-NMR and DRIFT spectroscopy. *European Journal of Soil Science*, *48*(2), 301–310. https://doi.org/10.1111/j.1365-2389.1997.tb00550.x

Kaplan, D. I., Xu, C., Huang, S., Lin, Y., Tolić, N., Roscioli-Johnson, K. M., et al. (2016). Unique organic matter and microbial properties in the rhizosphere of a wetland soil. *Environmental Science and Technology*, *50*(8), 4169–4177. https://doi.org/10.1021/acs.est.5b05165

Kappler, A., Benz, M., Schink, B., & Brune, A. (2004). Electron shuttling via humic acids in microbial iron(III) reduction in a freshwater sediment. *FEMS Microbiology Ecology*, *47*(1), 85–92. https://doi.org/10.1016/S0168-6496(03)00245-9

Knorr, K. H., Lischeid, G., & Blodau, C. (2009). Dynamics of redox processes in a minerotrophic fen exposed to a water table manipulation. *Geoderma*, *153*(3–4), 379–392. https://doi.org/10.1016/j.geoderma.2009.08.023

Kramer, M. G., & Chadwick, O. A. (2018). Climate-driven thresholds in reactive mineral retention of soil carbon at the global scale. *Nature Climate Change*, *8*(12), 1104–1108. https://doi.org/10.1038/s41558-018-0341-4

Lentini, C. J., Wankel, S. D., & Hansel, C. M. (2012). Enriched iron(III)-reducing bacterial communities are shaped by carbon substrate and iron oxide mineralogy. *Frontiers in Microbiology*, *3*, 1–19. https://doi.org/10.3389/fmicb.2012.00404

Loheide, S. P., Deitchman, R. S., Cooper, D. J., Wolf, E. C., Hammersmark, C. T., & Lundquist, J. D. (2008). A framework for understanding the hydroecology of impacted wet meadows in the Sierra Nevada and Cascade Ranges, California, USA. *Hydrogeology Journal*, *17*(1), 229–246. https://doi.org/10.1007/s10040-008-0380-4

Loheide, S. P., & Gorelick, S. M. (2007). Riparian hydroecology: A coupled model of the observed interactions between groundwater flow and meadow vegetation patterning. *Water Resources Research*, *43*(7), 1–16. https://doi.org/10.1029/2006WR005233

Louca, S., Parfrey, L. W., & Doebeli, M. (2016). Decoupling function and taxonomy in the global ocean microbiome. *Science*, *353*(6305), 1272–1277. https://doi.org/10.1126/science.aaf4507

Louca, S., Polz, M. F., Mazel, F., Albright, M. B. N., Huber, J. A., O'Connor, M. I., et al. (2018). Function and functional redundancy in microbial systems. *Nature Ecology and Evolution*, *2*(6), 936–943. https://doi.org/10.1038/s41559-018-0519-1

Lovley, D. R. (1987). Organic matter mineralization with the reduction of ferric iron: A review. *Geomicrobiology Journal*, *5*(3), 375–399. https://doi.org/10.1080/01490458709385975

Lovley, D. R., Coates, J. D., Blunt-Harris, E. L., Phillips, E. J. P., & Woodward, J. C. (1996). Humic substances as electron acceptors for microbial respiration. *Nature*, *382*(6590), 445–448. https://doi.org/10.1038/382445a0

Lovley, D. R., & Holmes, D. E. (2004). Dissimilatory Fe (III) and Mn (IV) reduction. *Advances in Microbial Physiology*, *55*(2), 220–286. https://doi.org/10.1128/mr.55.2.259-287.1991

Lovley, D. R., & Phillips, E. J. P. (1987). Rapid assay for microbially reducible ferric iron in aquatic sediments. *Applied and Environmental Microbiology*, *53*(7), 1536–1540. https://doi.org/10.1128/aem.53.7.1536-1540.1987

Lovley, D. R., & Phillips, E. J. P. (1988). Novel mode of microbial energy metabolism: Organic carbon oxidation coupled to dissimilatory reduction of iron or manganese. *Applied and Environmental Microbiology*, *54*(6), 1472–1480. https://doi.org/10.1128/aem.54.6.1472-1480.1988

McNicol, G., & Silver, W. L. (2014). Separate effects of flooding and anaerobiosis on soil greenhouse gas emissions and redox sensitive biogeochemistry. *Journal of Geophysical Research: Biogeosciences*, *119*(4), 557–566. https://doi.org/10.1002/2013JG002433

Merino, C., Kuzyakov, Y., Godoy, K., Cornejo, P., & Matus, F. (2020). Synergy effect of peroxidase enzymes and Fenton reactions greatly increase the anaerobic oxidation of soil organic matter. *Scientific Reports*, *10*(1), 1–12. https://doi.org/10.1038/s41598-020-67953-z

Morra, B., Brisbin, H., Stringham, T., & Sullivan, B. W. (2023). Ecosystem carbon and nitrogen gains following 27 years of grazing management in a semiarid alluvial valley. *Journal of Environmental Management*, *337*, 117724. https://doi.org/10.1016/j.jenvman.2023.117724

National Fish and Wildlife Foundation. (2010). Sierra Nevada meadow restoration business plan.

Nelson, M. B., Martiny, A. C., & Martiny, J. B. H. (2016). Global biogeography of microbial nitrogen-cycling traits in soil. *Proceedings of the National Academy of Sciences of the United States of America*, *113*(29), 8033–8040. https://doi.org/10.1073/pnas.1601070113

Norton, J. B., Jungst, L. J., Norton, U., Olsen, H. R., Tate, K. W., & Horwath, W. R. (2011). Soil carbon and nitrogen storage in upper montane riparian meadows. *Ecosystems*, *14*(8), 1217–1231. https://doi.org/10.1007/s10021-011-9477-z

Norton, J. B., Olsen, H. R., Jungst, L. J., Legg, D. E., & Horwath, W. R. (2014). Soil carbon and nitrogen storage in alluvial wet meadows of the Southern Sierra Nevada Mountains, USA. *Journal of Soils and Sediments*, *14*(1), 34–43. https://doi.org/10.1007/s11368-013-0797-9

Oksanen, J., Blanchet, F. G., Friendly, M., Kindt, R., Legendre, P., McGlinn, D., et al. (2018). vegan: Community Ecology Package. R package version 2 (pp. 5–3).

Pan, W., Kan, J., Inamdar, S., Chen, C., & Sparks, D. (2016). Dissimilatory microbial iron reduction release DOC (dissolved organic carbon) from carbon-ferrihydrite association. *Soil Biology and Biochemistry*, *103*, 232–240. https://doi.org/10.1016/j.soilbio.2016.08.026

Patzner, M. S., Kainz, N., Lundin, E., Barczok, M., Smith, C., Herndon, E., et al. (2022). Seasonal fluctuations in iron cycling in thawing permafrost peatlands. *Environmental Science and Technology*, *56*(7), 4620–4631. https://doi.org/10.1021/acs.est.1c06937

Patzner, M. S., Mueller, C. W., Malusova, M., Baur, M., Nikeleit, V., Scholten, T., et al. (2020). Iron mineral dissolution releases iron and associated organic carbon during permafrost thaw. *Nature Communications*, *11*(1), 1–11. https://doi.org/10.1038/s41467-020-20102-6

PRISM Climate Group. (2010). *30-Year normals; 1981-2010*. Oregon State University. Retrieved from http://prism.oregonstate.edu

R Core Team. (2017). *R: A language and environment for statistical computing*. R Foundation for Statistical Computing.

R Core Team. (2020). *R: A language and environment for statistical computing*. R Foundation for Statistical Computing. Retrieved from https://www.r-project.org/

Reed, C. C., Berhe, A. A., Moreland, K. C., Wilcox, J., & Sullivan, B. W. (2022). Restoring function: Positive responses of carbon and nitrogen to 20 years of hydrologic restoration in montane meadows. *Ecological Applications*, *32*(7), e2677. https://doi.org/10.1002/eap.2677

Reed, C. C., Merrill, A. G., Drew, W. M., Christman, B., Hutchinson, R. A., Keszey, L., et al. (2021). Montane meadows: A soil carbon sink or source? *Ecosystems*, *24*(5), 1125–1141. https://doi.org/10.1007/s10021-020-00572-x

Roden, E. E., & Urrutia, M. M. (2002). Influence of biogenic Fe(II) on bacterial crystalline Fe(III) oxide reduction. *Geomicrobiology Journal*, *19*(2), 209–251. https://doi.org/10.1080/01490450252864280

Roden, E. E., & Wetzel, R. G. (1996). Organic carbon oxidation and suppression of methane production by microbial Fe(III) oxide reduction in vegetated and unvegetated freshwater wetland sediments. *Limnology & Oceanography*, *41*(8), 1733–1748. https://doi.org/10.4319/lo.1996.41.8.1733

Roden, E. E., & Wetzel, R. G. (2002). Kinetics of microbial Fe(III) oxide reduction in freshwater wetland sediments. *Limnology & Oceanography*, *47*(1), 198–211. https://doi.org/10.4319/lo.2002.47.1.0198

Saidy, A. R., Smernik, R. J., Baldock, J. A., Kaiser, K., Sanderman, J., & Macdonald, L. M. (2012). Effects of clay mineralogy and hydrous iron oxides on labile organic carbon stabilisation. *Geoderma*, *173–174*, 104–110. https://doi.org/10.1016/j.geoderma.2011.12.030

Schloss, P. D., Westcott, S. L., Ryabin, T., Hall, J. R., Hartmann, M., Hollister, E. B., et al. (2009). Introducing mothur: Open-source, platform-independent, community-supported software for describing and comparing microbial communities. *Applied and Environmental Microbiology*, *75*(23), 7537–7541. https://doi.org/10.1128/AEM.01541-09

Shields, M. R., Bianchi, T. S., Gélinas, Y., Allison, M. A., & Twilley, R. R. (2016). Enhanced terrestrial carbon preservation promoted by reactive iron in deltaic sediments. *Geophysical Research Letters*, *43*(3), 1149–1157. https://doi.org/10.1002/2015GL067388

Shrestha, J., Rich, J. J., Ehrenfeld, J. G., & Jaffe, P. R. (2009). Oxidation of ammonium to nitrite under iron-reducing conditions in wetland soils: Laboratory, field demonstrations, and push-pull rate determination. *Soil Science*, *174*(3), 156–164. https://doi.org/10.1097/SS.0b013e3181988fbf

Sidhu, P. S., Gilkes, R. J., Cornell, R. M., Posner, A. M., & Quirk, J. P. (1981). Dissolution of iron oxides and oxyhydroxides in hydrochloric and perchloric acids. *Clays and Clay Minerals*, *29*(4), 269–276. https://doi.org/10.1346/CCMN.1981.0290404

Stookey, L. L. (1970). Ferrozine - a new spectrophotometric reagent for iron. *Analytical Chemistry*, *42*(7), 779–781. https://doi.org/10.1021/ac60289a016

Torn, M. S., Trumbore, S. E., Chadwick, O. A., Vitousek, P. M., & Hendricks, D. M. (1997). Mineral control of soil organic carbon storage and turnover. *Nature*, *389*(6647), 170–173. https://doi.org/10.1038/38260

Wagai, R., & Mayer, L. M. (2007). Sorptive stabilization of organic matter in soils by hydrous iron oxides. *Geochimica et Cosmochimica Acta*, *71*(1), 25–35. https://doi.org/10.1016/j.gca.2006.08.047

Wan, D., Ye, T., Lu, Y., Chen, W., Cai, P., & Huang, Q. (2019). Iron oxides selectively stabilize plant-derived polysaccharides and aliphatic compounds in agricultural soils. *European Journal of Soil Science*, *70*, 1153–1163. https://doi.org/10.1111/ejss.12827

Wang, H., River, M., & Richardson, C. J. (2019). Does an "iron gate" carbon preservation mechanism exist in organic-rich wetlands? *Soil Biology and Biochemistry*, *135*, 48–50. https://doi.org/10.1016/j.soilbio.2019.04.011

Wang, Y., Wang, H., He, J. S., & Feng, X. (2017). Iron-mediated soil carbon response to water-table decline in an alpine wetland. *Nature Communications*, *8*, 1–9. https://doi.org/10.1038/ncomms15972

Wen, Y., Zang, H., Ma, Q., Chadwick, D. R., Evans, C. D., Chadwick, D. R., & Jones, D. L. (2019). Is the "enzyme latch" or "iron gate" the key to protecting soil organic carbon in peatlands? *Geoderma*, *349*, 107–113. https://doi.org/10.1016/j.geoderma.2019.04.023

Wiseman, C. L. S., & Pü, W. (2006). Interactions between mineral phases in the preservation of soil organic matter. *Geoderma*, *134*(1–2), 109–118. https://doi.org/10.1016/j.geoderma.2005.09.001

Wood, S. H. (1975). *Holocene stratigraphy and chronology of mountain meadows*. California Institute of Technology.

Yang, W. H., Weber, K. A., & Silver, W. L. (2012). Nitrogen loss from soil through anaerobic ammonium oxidation coupled to iron reduction. *Nature Geoscience*, *5*(8), 538–541. https://doi.org/10.1038/ngeo1530

Yao, Z., Wang, C., Song, N., Wang, C., & Jiang, H. (2020). Oxidation of ammonium in aerobic wastewater by anoxic ferric iron-dependent ammonium oxidation (Feammox) in a biofilm reactor. *Desalination and Water Treatment*, *173*(3), 197–206. https://doi.org/10.5004/dwt.2020.24822

Yu, G. H., & Kuzyakov, Y. (2021). Fenton chemistry and reactive oxygen species in soil: Abiotic mechanisms of biotic processes, controls and consequences for carbon and nutrient cycling. *Earth-Science Reviews*, *214*, 103525. https://doi.org/10.1016/j.earscirev.2021.103525

Zhu, J., Yan, X., Zhou, L., Li, N., Liao, C., & Wang, X. (2022). Insight of bacteria and archaea in Feammox community enriched from different soils. *Environmental Research*, *203*, 111802. https://doi.org/10.1016/j.envres.2021.111802